

PAPER • OPEN ACCESS

Evaluation of AHSS concepts with a focus on the product properties and appropriate casting characteristics of *Arvedi ESP thin slab casters*

To cite this article: C. Bernhard *et al* 2019 *IOP Conf. Ser.: Mater. Sci. Eng.* **529** 012071

View the [article online](#) for updates and enhancements.



IOP | ebooks™

Bringing you innovative digital publishing with leading voices to create your essential collection of books in STEM research.

Start exploring the [collection](#) - download the first chapter of every title for free.

Evaluation of AHSS concepts with a focus on the product properties and appropriate casting characteristics of *Arvedi ESP thin slab casters*

C. Bernhard¹, B. Linzer², P. Presoly¹, I. Watzinger², J. Watzinger²

¹ Montanuniversitaet Leoben, Franz-Josef-Strasse 18, 8700 Leoben, Austria

² Primetals Technologies Austria GmbH, Turmstraße 44, 4031 Linz, Austria

Abstract. The Arvedi ESP process and a variety of produced materials have been continuously developed since the opening of the Arvedi ESP plant in Cremona in 2009 to meet market demands for more sophisticated steel grades. The development of grades for more advanced applications such as advanced high strength steels and multiphase grades is of interest. Dual phase grades such as DP600 are already produced through an ESP line on an industrial scale; additional multi-phase grades such as TRIP are under development. High-strength steels for the automotive industry have especially high demands on material properties. In addition to the mechanical material properties, an excellent surface quality is required. The fundamental basis for such material properties on rolled coils needs to be provided from continuous casting. This paper deals with the classification of different – either Si- or Al-based – alloying concepts for TRIP steels with respect to their prospective behaviour in a thin slab caster.

1. Introduction

Advanced high-strength steels (AHSS) are the most cost-effective lightweight alternative for mass produced vehicles. The global demand for AHSS is expected to increase by nearly 100 % between 2017 and 2025 according to estimates [1]. In cars, TRIP steels are mainly used for structural and reinforcement parts (e.g., B-pillar uppers, roof rails, and front rails), typically in strip gauges of 1.2 – 2 mm and are mostly produced via cold rolling and subsequent hot-dip galvanizing or continuous annealing.

Providing satisfying shape tolerances and microstructure homogeneity in hot rolled strips with thickness of 1.5 mm offers a cost-efficient alternative to cold-rolled TRIP steel on the market. Among the commercialized thin slab casting and direct rolling (TSDR) concepts, the Arvedi endless strip production (ESP) process has the highest potential to stably produce AHSS steel grades.

Steel grades such as DP 600 and DP 800 are commonly used and are frequently provided by TSDR processes. Manufacturing such products on an ESP line confirmed that the unique stable production conditions offered by the endless process are superior to those of batch processes [25].

Supporting the advantages of the Arvedi-ESP-process, **Figure 1** shows an excerpt of a DP 600 production sequence. The temperature control on the run-out table can be adjusted in a very accurate manner to obtain the correct microstructure as defined by phase selection and grain sizes and can be controlled afterwards for several hours with very minor deviations. The separation between the coils is achieved by using shear directly in front of the down coilers, which has no influence on the entire upstream process. With such production conditions, the pass schedules for the rolling mill part can be selected in a more optimized way to allow for products with width, thickness, shape and flatness



comparable to conventionally cold rolled material. Threading and tailing out is eliminated, and the rolling parameters show similar stability characteristics to the given examples regarding temperature, which is in accordance with the typically higher requirements for the process conditions and narrowed production parameter fields of the steel grades of interest.

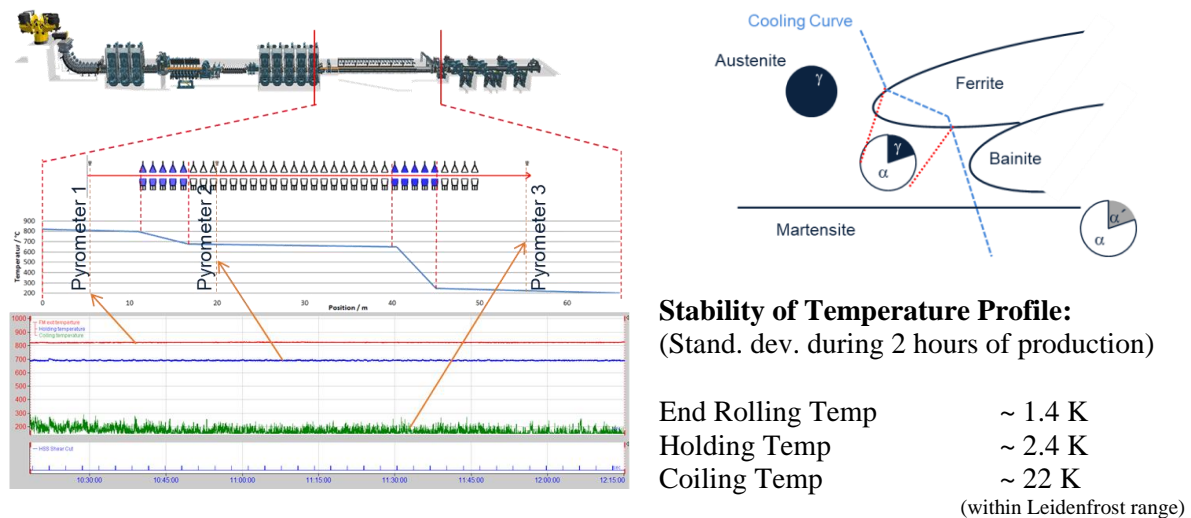


Figure 1: Cooling pattern and temperature readings of pyrometers at the run-out table area during a two-hour production sequence (approx. 700 t) of DP 600 steel from an ESP line.

The present work focusses on the evaluation of common TRIP steel concepts with regard to the casting characteristics in an Arvedi ESP thin slab caster.

2. TRIP steels: Common alloying concepts

TRIP steels typically consist of a multiphase microstructure with a ferritic matrix, bainite, retained austenite and some martensite. The TRIP effect arises during plastic deformation and results in an outstanding combination of strength and total elongation.

The TRIP microstructure can either be achieved after hot rolling or for cold rolled strip, after continuous annealing or hot dip galvanizing. In hot rolling, the multiphase microstructure develops after the austenitic rolling by multistage cooling at the run-out table and coiler, which is rather difficult to control [e.g., 6]. Continuous annealing and hot dip galvanizing provide a multiphase microstructure through a two-stage heat treatment, including intercritical annealing above the Ar1 temperature to adjust a certain volume fraction of ferrite and, after accelerated cooling to the isothermal holding temperature, the partial transformation of austenite to bainite, which provides the partitioning of carbon and thus leads to the stabilization of the retained austenite at room temperature.

The classic alloying concept of TRIP steels contains 0.2 wt.% C, 1.0-2.0 wt.% Si and 1.5-2.0 wt.% Mn. These steels are henceforth referred to as “*high-Si concept*” [2-5]. The main role of Si in this concept is to suppress the precipitation of carbides from the austenite. In addition, Si contributes to the strength of TRIP steels by solid-solution hardening. In contrast to the positive effects of Si, Si is also known to cause inner oxidation at elevated temperatures and causes hot-dip galvanizing problems [13].

The replacement of Si by other elements is thus an important issue in TRIP steel development, and Al is widely used today [8-14]. Al is a strong ferrite forming element but cannot fully replace Si, as Si more effectively suppresses cementite precipitation. In addition, Al does not significantly contribute to solution strengthening. Hence, low Si - “*high-Al concepts*” with typically 1.2 – 1.7 wt.% Al often contain microalloying elements such as Nb and V to increase the strength from precipitation hardening [e.g., 8, 9]. The main problem in the production of a steel with such a high Al content via the continuous casting

process is the interaction between the steel and mould flux [19-22]. The reduction of chemically less stable oxides at the steel/flux interface by the dissolved Al and the separation of Al_2O_3 from the steel into the flux result in a significant increase in the Al_2O_3 content in the mould flux with increasing casting time. These effects cause steadily increasing viscosity and poor lubrication between the strand and the mould and may ultimately result in break-outs and deterioration of the surface quality.

An alternative ferrite stabilizer is phosphorus. P is highly effective at suppressing carbide precipitation and contributes to strength via solute solution strengthening. Thus far, TRIP steel concepts with up to 0.1 wt.% P have been investigated [10, 11, 13, 14]. In casting, phosphorus is a rather critical element; P is one of the strongest segregating elements and may cause problems with internal cracking [15]. Additionally, grain boundary segregation may cause embrittlement at lower temperatures and during annealing.

In summary, all available ferrite stabilizers have associated problems in the production route: high Si content is critical for galvanizing and heat treatment, whereas high Al and P contents are critical to the casting process. Therefore, a common strategy is to combine reduced Si and Al contents to achieve the TRIP microstructure. Si contents of approximately 0.5 wt.% and Al contents of 0.8 – 1.0 wt.% are typical for the “*Si-Al concepts*”. The addition of microalloying elements such as Nb has also been proposed [8, 9].

With respect to the behaviour of TRIP concepts in a thin slab caster, three concepts were selected for detailed investigations, the chemical compositions of which are given in **Table 1**:

- a high-Si concept similar to [6] but without Nb and Ti,
- a Si-Al concept slightly modified from [8],
- and a high-Al concept according to [12].

Samples with a weight of 300 g were melted in a Linn High Therm Lifumat high-frequency re-melting and fusion unit. The melts were prepared under argon atmosphere from high-purity raw-materials in an alumina crucible. The samples were characterized by excellent homogeneity due to rapid solidification in a copper mould and thus provided perfect testing materials for thermal analysis and all other laboratory experiments.

Several aspects of the prospective behaviour of the three alloying concepts for thin slab casting were investigated in experiments and theoretical considerations including:

- the phase transformation sequence during solidification to determine whether the alloying concept is hypo-peritectic or hyper-peritectic,
- the surface scale formation and tendency towards inner oxidation and the resulting risk for the formation of surface defects, and
- the sensitivity to the formation of internal defects and the homogeneity of the semi-finished product.

The results are discussed in detail in the following sections.

Table 1. TRIP steel concepts from literature used for further investigation.

No.	Wt.%C	Wt.%Si	Wt.%Mn	Wt.%Al	Others all in wt.%
High-Si concept	0.18	1.47	1.60	0.033	
Si-Al concept	0.20	0.50	1.46	0.68	each element < 0.01 %
High-Al concept	0.15	0.02	1.52	1.40	

3. Phase transformations during solidification in equilibrium

It is well-known that hypo-peritectic steels are extremely prone to the formation of defects in continuous casting [e.g., 18]: The uneven initial solidification due to the shrinkage induced by the phase transformation from ferrite to austenite immediately next to the solidus results in unsteady heat transfer

in the meniscus region and mould level fluctuations. In addition, hypo-peritectics show a tendency to form deep oscillation marks. In consequence, peritectic steels are highly sensitive to the formation of internal defects and surface defects in the casting process. The number of countermeasures is limited and among them, the use of mould fluxes with low viscosity and high break temperature to reduce the heat transfer close to the meniscus is the most promising [18]. Due to these numerous casting problems, peritectic steels are generally considered unfavourable for high-speed casting in TSDR plants.

Thermal analysis by differential thermal analysis (DTA) and differential scanning calorimetry (DSC) were the most effective methods to accurately characterize the phase transformation sequence in the high temperature range. The DTA/DSC signal-based classification of Fe-alloys as hypo-peritectic, hyper-peritectic or low carbon steel correlates well with plant data, although the results apply only to equilibrium [16]. In the plant, hypo-peritectics are easy to identify by means of the measured temperature in the mould and the determined temperature variation coefficient [18]. A further finding from extensive DTA/DSC measurements was the apparent inaccuracy of commercial databases for the Fe-C-Si-Mn system [17] and for elevated Al content in the Fe-C-Mn-Al system, both of the highest importance for TRIP steel grades.

The available DTA/DSC-data was used to locally assess the SGTE alloy database for the system Fe-C-Mn-Si-Al [17]. This database excerpt was used to predict the influences of Si and Al on the hypo-peritectic range depending on carbon and manganese contents, as shown in **Figures 2a and 2b**. The classic high-Si concepts with 0.2 wt.% C are clearly located in the hyper-peritectic range, which also applies to the Si-Al concept. In general, the role of Si as a ferrite former in solidification of Fe-alloys is widely overestimated. Al is by far more effective, and for 0.2 wt.% C, an excess of approximately 1.3 wt.% Al results in hypo-peritectic solidification. Lowering the carbon content is, with respect to the castability, also a critical measure; the high-Al alloy is explicitly a hypo-peritectic steel and is unfavourable for thin slab casting. The role of P was not explicitly addressed in these calculations.

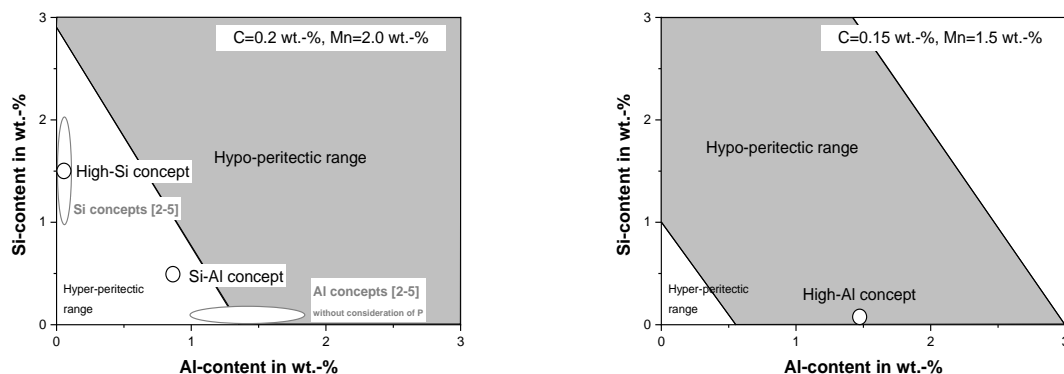


Figure 2a. Hypo-peritectic range for 0.2 wt.% C and 2.0 wt.% Mn depending on Al and Si contents.

Figure 2b. Hypo-peritectic range for 0.15 wt.% C and 1.5 wt.% Mn depending on Al and Si contents.

Another key aspect for the casting of TRIP steels in a thin slab caster that is not thoroughly described here is the mould flux. In the casting of high-Al steel grades, SiO_2 and other less stable oxides are reduced by the dissolved Al in the steel, and the Al_2O_3 content in the flux accumulates [e.g., 19]. This effect results in increasing viscosity, decreasing mould flux consumption and a change in the primary crystallizing phase. The final consequences are unstable heat extraction, stronger slag rim, lower slag consumption, uneven shell growth resulting in poor surface quality and the occurrence of break-outs. Plant observations report an increase in Al_2O_3 in the flux to between 15 and 35 wt.% depending on the Al content of the steel and the mould flux concept [20 - 22]. The Al_2O_3 accumulation rate depends on the dissolved Al content as long as the Al content is below 2 wt.%. The accumulation rate decreases significantly as soon as the Al content decreases to 0.5 wt.%.

With respect to sufficient lubrication in the mould, maximum Al contents between 0.5 and 0.8 % should not be exceeded to prevent an uncontrollable increase of Al_2O_3 in the mould flux.

4. Surface oxidation and surface defect formation

High-Si AHSS steels are well known to form highly adherent surface scales during casting and further processing. The main reason for these scales is the formation of a low melting FeO-2FeO-SiO_2 eutectic with a melting point below $1200\text{ }^\circ\text{C}$ [24]. In Si-Al-AHSS concepts, the liquid phases close to the interface consist of $\text{Al}_2\text{O}_3\text{-SiO}_2\text{-FeO}_n$ [25]. Even high-pressure hydraulic descaling has difficulty removing this oxide layer from the surface of the cast product. An additional phenomenon is selective oxidation along the grain boundaries and inner oxidation, i.e., the formation of oxides at the steel/scale interface. The high-Si TRIP concepts must therefore be critically evaluated with respect to the achievable surface quality of the hot rolled strip.

The oxidation of the three alloying concepts with the composition given in **Table 1** was simulated in a Netzsch STA 409 PG under simplified conditions, as shown in **Figure 3a**. The samples were heated under Ar-6.0 flushing, and after reaching a temperature of $1200\text{ }^\circ\text{C}$ and temperature equalization, air was supplied to the furnace for 2 or 10 minutes before switching back to Ar 6.0 protection during cooling. Two thermal cycles were applied: cooling from 1200 to $1100\text{ }^\circ\text{C}$ in either 2 minutes or 10 minutes, simulating the cooling in a thin slab caster (“ESP-cycle”) or a conventional caster (“CC cycle”). The results give only a qualitative indication of the behaviour of the three alloying concepts with respect to scale formation and inner oxidation.

Figure 3b shows the final mass change of the samples due to the oxidation. The oxidation seems to mainly depend on the Si content of the sample, and the results confirm the role of Al as an inhibitor for oxidation [24]. The oxidation after 2 minutes is by far lower than that for 10 minutes of oxidation.

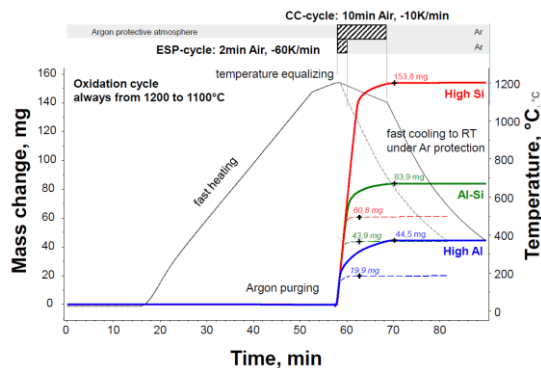


Figure 3a. Thermal cycle and mass change vs. time for the performed measurements

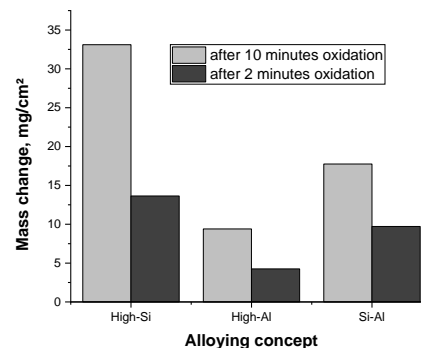


Figure 3b. Mass change of the sample after the oxidation experiments

Figures 4a-4f summarize the SEM results for the six measurements; the left side shows results after two minutes of oxidation, and the right side shows results after 10 minutes of oxidation. The magnification is identical for each of the micrographs. For the high Si concept, deep penetration of a mixture of SiO_2 and $\text{FeO/Fe}_2\text{O}_3$ along the former austenite grain boundaries becomes clearly visible. In the scale/bulk-interface, SiO_2/MnO particles nucleate. The scale layer closest to the interface consists of a FeO-2FeO-SiO_2 mixture with characteristics of a formerly liquefied layer. The oxide layer adheres to the interface after the experiment.

The oxidation of the high-Al samples results in the formation of an $\text{Al}_2\text{O}_3/\text{MnO/FeO}_n$ layer surrounding the former austenite grains. The oxide particles in the bulk have a similar composition. The former austenite grains are very small in diameter, indicating the strong pinning effect of the AlN precipitations. The thickness of the interface layer increases over time.

For the Si-Al concept, the oxide particles in the interface layer consist mainly of Al_2O_3 and MnO . It is surprising that no significant enrichment of Al or Si along the former grain boundaries is detectable and that the whole interface is nearly free from any significant enrichment of Si. Only the first oxide scale layers contain a significant amount of SiO_2 .

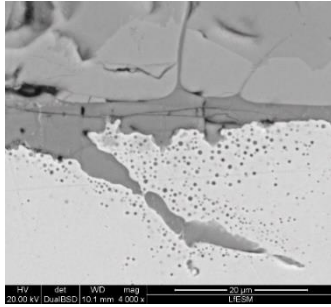


Figure 4a. High-Si concept, 2 minutes

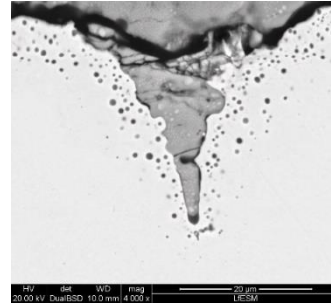


Figure 4b. High-Si concept, 10 minutes

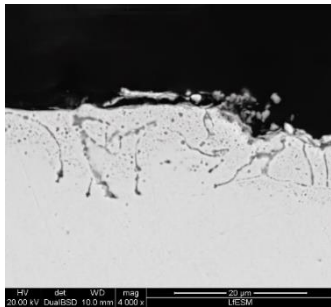


Figure 4c. High-Al concept, 2 minutes

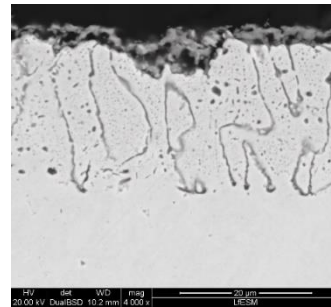


Figure 4d. High-Al concept, 10 minutes

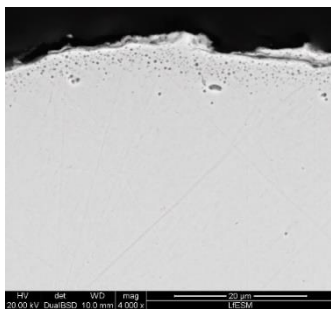


Figure 4e. Si-Al concept, 2 minutes

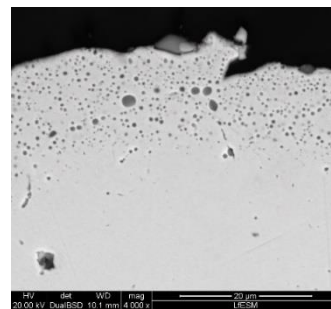


Figure 4f. Si-Al concept, 10 minutes

The adherence of the oxide layer after the experiment is very low for the high-Al and Si-Al-alloys; the oxide layer dropped off the samples from only handling after removing the samples from the TG. Even if the results provide only qualitative indications, the results confirm that a high-Si concept is critical for TSDR plants due to the formation of a highly adherent scale and a deep penetration of the interface by oxide layers. The lower time at higher temperature for the “ESP-cycle” (2 minutes of oxidation) greatly improves the oxidation. The Si-Al concept seems to receive the most benefit, and the risk of the formation of surface defects due to the rolling in of adhered scale or oxide-penetrated grain boundaries seems to be rather low.

5. Internal defects and homogeneity

Regarding the formation of internal defects such as hot tear segregations, microsegregation is a key factor. The most common approach for predicting these kinds of defects in continuous casting is a strain criterion. The deformation of the strand by bending, straightening and bulging between the supporting rolls causes tensile strain in the two-phase liquid/solid region. Under the assumption of columnar growth of dendrites, which is a given for high-speed thin slab casting of steel, the straining by every pair of rolls is accumulated in a so-called *critical temperature range* (CTR). For the CTR, the temperature ranges between the defined solid fractions and solid fractions of 0.8 (or 0.9) and 1.0 (or 0.99) are frequently used as the upper and lower limits [e.g., 27]. For the following hot tearing analysis, the range of preferred strain accumulation (ΔT_A) is defined as $f_s = 0.96 - 1.0$ [26]. The corresponding solidus temperatures are calculated with a numerical solution of Ohnaka's microsegregation model in ChemApp under the assumption of local (temperature dependant) equilibrium partition coefficients from the optimized FactSAGE Fe-C-Mn-Si-Al database [28]. The resultant temperatures and ΔT_A are listed in **Table 2**. Together with the three selected samples, the Al-P concept according to [13] was analysed. In addition to carbon and manganese, Si has a noticeable decreasing effect on the solidus temperature, at least in the high-Si concept. The influence of Al on the solidus is negligible, whereas P has a strong decreasing influence on the solidus as expected.

Table 2. Solidus temperatures for TRIP steel concepts, cooling rate 1 K/s.

No.	$T(f_s = 0.96)$ °C	$T(f_s = 1.0)$ °C	ΔT_A
High-Si concept	1432.3	1418.9	13.4
Si-Al concept	1453.1	1443.1	10.0
High-Al concept	1478.4	1470.1	8.3
Al-P concept [13]	1448.9	1427.7	21.2

The analysis of the hot tearing bases in the numerical simulation of solidification in a thin slab caster (casting speed 5 m/min, cooling for medium carbon steel, thickness in run-out area is 95 mm). The strain rate caused by bulging, liquid core reduction and straightening is predicted by a frequently used empirical formula [e.g., 27] and accumulated in the temperature range of preferred strain accumulation ΔT_A . The solidification is considered by the shell growth velocity of the solidus isotherm R_S and the temperature gradient between the liquidus and solidus G_{LS} . **Formula 1** summarizes this simplified approach for a strain rate-based hot tearing criterion. The critical strain ε_{crit} is determined from SSCT (submerged split-chill tensile) experiments according to [26]. For the presented analysis, the critical strain was assumed as 1.6 % for the Si and Al concept and as 1.0 % for the Al-P concept.

$$\Delta T_A \cdot \dot{\varepsilon} \cdot (R_S G_{LS})^{-1} < \varepsilon_{crit} \quad (1)$$

Figure 5a shows the calculated temperature of the surface and the temperatures at defined distances from the surface together with the calculated shell growth. **Figure 5b** summarizes the results of the hot tearing analysis: if the ratio between the maximum accumulated strain ε_{accum} and the critical strain ε_{crit} exceeds 1, the formation of hot tears under the assumed conditions is likely, as is the case for the Al-P concept due to the strong microsegregation of P. Among all the considered concepts, the Al concept is the least sensitive to hot tearing, but in general, the investigated steel grades should not be susceptible to hot tearing unless the phosphorus content is increased.

The analysis described above is only one-dimensional, but the results are significant for the general classification of steel grades regarding internal defect formation for a given caster design and defined

operation conditions. Tensile strain may also be localized by the deformation of the shell in two dimensions, such as in liquid core reduction (LCR). LCR is a necessity for TSDR technologies when the thickness of the cast thin slab has to be reduced before the first rolling passes. The Arvedi ESP concept is based on the casting of 95 mm strand thickness and LCR of only a few millimetres, as the high hot forming potential of the high reduction mill makes higher reductions within the caster obsolete. This result is another way that Arvedi ESP presents excellent prerequisites for the casting of AHSS grades.

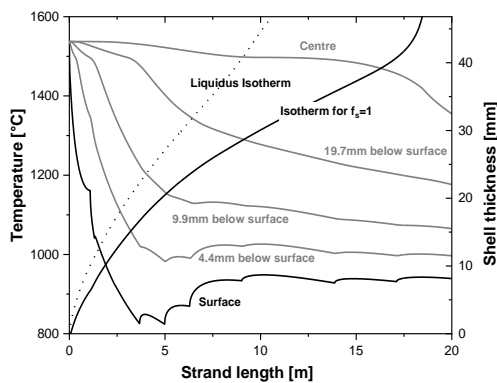


Figure 5a. Shell growth for thin slab caster, 5 m/min, 95 mm slab thickness.

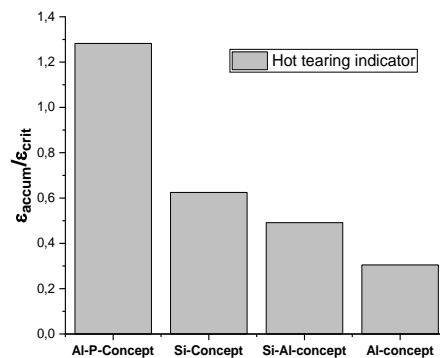


Figure 5b. Hot tearing indicator $\epsilon_{accum}/\epsilon_{crit}$ for the four selected steel grades.

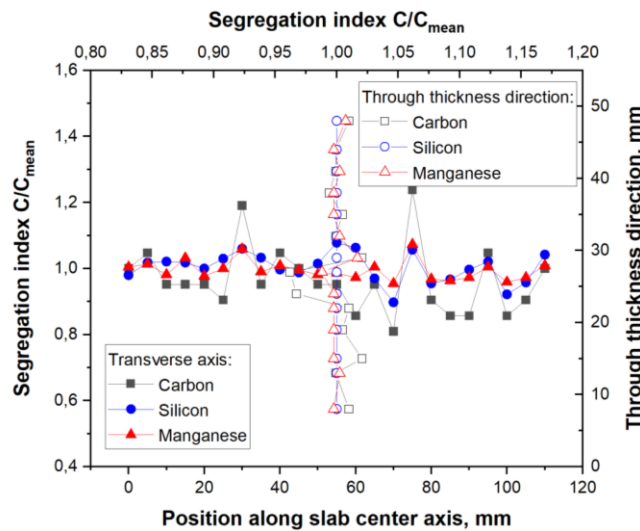


Figure 6. Local segregation index C/C_{mean} along centre axis and across the thickness of a thin slab.

The last aspect that is addressed by this study is the enrichment of alloying elements at the macroscopic scale. The demands on the homogeneity of the strip after hot rolling are high, and the prevention of pronounced centre segregation and a resulting banded structure in the hot rolled strip must be considered crucial. **Figure 6** presents the OES-measured concentrations of carbon, silicon and manganese for a thin slab from a plant trial (0.2 wt.% carbon and 2.1 wt.% Mn steel; 5 m/min). The measurement was performed in the axial direction and the through thickness direction, and the absolute values are given

as the ratio between the local concentration and mean concentration (segregation index). The results show excellent Mn homogeneity with a minimum segregation index of 0.95 and a maximum of 1.07. The low diffusivity of Mn is a key factor for the homogeneity of the final product; neither holding at high temperature nor hot forming with the highest deformation significantly contributes to the homogenization of Mn, whereas the carbon concentration peaks are compensated during hot rolling due to the high diffusivity of carbon [29]. The ESP Arvedi thin slab therefore is an excellent material for the production of a homogeneous strip in the subsequent rolling process.

6. Conclusions

In the present work, three alloying concepts for TRIP steels were tested regarding their prospective behaviour in high-speed thin slab casting on an Arvedi ESP caster: a high-Al-grade, a high-Si-grade and a mixed Si-Al concept. The results showed that

- the *high-Al concept* is unsuitable due to the tendency towards hypo-peritectic solidification and the intensive chemical interaction with the mould fluxes. The oxidation of the high-Al-samples at temperatures between 1100 and 1200 °C results in grain boundary oxidation, which is a presumable reason for the formation of surface defects in the rolling process. The formation of internal cracks and inhomogeneity should be controllable due to the almost negligible enrichment of Al during solidification.
- The *high-Si concept* is hyper-peritectic and hence rather insensitive regarding the solidification in the mould. The oxidation experiments demonstrate the formation of a partly liquefied, adherent oxide layer, consisting of fayalite and associated with internal oxidation and selective oxidation along grain boundaries. This result could be an exclusion criterion for high-Si concepts. Si is a moderately segregating element and slightly increases the risk of the formation of internal cracks.
- The homogeneity of samples from plant trials is excellent, and the segregation indexes of Mn and Si close to the centre of the thin slab are almost equal to 1.
- *Phosphorus* is a rather unsuitable element to replace Si or Al as a ferrite former; the strong segregation results in a high risk for the formation of hot tears or overcritical centre segregations.
- The mixed *Si-Al concepts* show the highest potential among the investigated steel grades; hyper-peritectic solidification and a controllable interaction with the mould flux, the lowest tendencies towards inner oxidation and selective oxidation along grain boundaries and finally a low tendency towards the formation of internal defects provide an excellent basis for the further development of TRIP concepts for casting in thin slab casters.

7. Acknowledgements

Financial support by the Austrian Federal Government (in particular from Bundesministerium für Verkehr, Innovation und Technologie and Bundesministerium für Wirtschaft, Familie und Jugend) represented by Österreichische Forschungsförderungsgesellschaft mbH and the Styrian and the Tyrolean Provincial Government, represented by Steirische Wirtschaftsförderungsgesellschaft mbH and Standortagentur Tirol, within the framework of the COMET Funding Programme is gratefully acknowledged. This work is part of the ongoing K2-MPPE project P3.36 “Advanced ESP”.

8. References

- [1] Harris, T 2017 *SSAB Capital Markets Day* (www.SSAB.com)
- [2] Ryu H B, Speer J G and J P Wise 2002 *Met. Mat. Trans. A* **33A** 2811
- [3] Wu D, Zhuang L and H Lü 2008 *J. of Iron and Steel Research Int.* **15**(2) 65
- [4] Zhang Z, Zhu F and Y Li 2010 *J. of Iron and Steel Research Int.* **17**(7) 44
- [5] Zhang Y, Ma Y, Kang Y and H Yu 2006 *J. of Univ. Sci. Tech. Beijing* **13** 476

- [6] Liu J, Zhang Z, Zhu F, Li Y and K Manabe 2012 *J. of Iron and Steel Research Int.* **19**(1) 43
- [7] Timokhina I B, Pereloma E V and P D Hodgson 2001 *Mat. Sci. Tech.* **17** 135
- [8] Fu B, Yang, W Y, Lu M Y, Feng Q, Li L F and Z Q Sun 2012 *Mat. Sci. and Eng. A* **536** 265
- [9] Feng Q, Li L, Yang W and Z Sun 2014 *Mat. Sci. and Eng. A* **605** 14
- [10] Hou X, Xu Y, Zhao Y and D Wu 2011 *J. of Iron and Steel Research Int.* **18**(11) 40
- [11] Barbe L, Verbeken K and E Wettinck 2006 *ISIJ Int.* **48** 1251
- [12] Chen Y, Wang L, Dong L, Li F and Y Zhang 2007 *Proc. Sino-Swedish Structural Materials Symp.* 308
- [13] Ding W, Hedström P and Y Li 2016 *Mat. Sci. Eng. A* **674** 151
- [14] Jing C, Suh D W, Oh C S, Wang Z and S J Kim 2007 *Met. and Mat. Int.* **13**(1) 13
- [15] Pierer R and C Bernhard 2010 *Proc. AISTech* 193
- [16] Presoly P, Pierer R and C Bernhard 2012 *Proc. TMS* 299
- [17] Presoly P, Bernhard C and R Pierer 2012 *Met. Mat. Trans. A* **44** 5377
- [18] Xia G, Bernhard C, Ilie S and C Fürst 2011 *Steel research int.* **82** 230
- [19] Presoly P and C Bernhard 2017 *Iron & Steel Technology* **14** 100
- [19] Kim M S and Y B Kang 2018 *Calphad* **61** 115
- [20] Cho J W, Blazek K, Frazee M, Yin H B, Park J H and S W Moon 2013 *ISIJ Int.* **53** 62
- [21] Harmuth H and G Xia 2014 *Prod. 8th European Cont. Casting Conf.* Graz/Austria
- [22] Rudnitzki J, Shepherd R, Balichev E, Karrasch S and F Krueger 2014 *Prod. 8th European Cont. Casting Conf.* Graz/Austria
- [23] Sauerhammer B, Senk D, Schmidt E, Safi M, Spiegel M and S Sridhar 2006 *Met. Mat. Trans.* **36B** 503
- [24] Takeda M, Onishi T, Nakakubo S and S Fujimoto 2009 *Mat. Trans.* **9** 2242
- [25] Bragin S, Großeiber S, Linzer B and A Rimnac, 2016 *Proc. 10th Intern. Rolling Conf. and 7th Europ. Rolling Conf.* Graz/Austria
- [26] Bernhard C and R Pierer Proc. 2007 *Proc. 5th Decennial International Conference on Solidification Processing* Sheffield, UK 525
- [27] Won Y M, Yeo T J, Seol D J and K H Oh 2000 *Met. Mat. Trans.* **31B** 779
- [28] You D, Bernhard C, Wieser G and S Michelic 2016 *Steel research int.* **87** 840
- [29] Presslinger H, Ilie S, Schiefermueller A, Pissenberger A, Parteder E and C Bernhard 2006 *ISIJ Int.* **46** 1845